Appl Nanosci (2014) 4:531–536
DOI 10.1007/s13204-013-0231-z

ORIGINAL ARTICLE

Structural, optical and ferroelectric properties of V doped ZnO

Rahul Joshi · Parmod Kumar · Anurag Gaur · K. Asokan

Received: 30 January 2013 / Accepted: 6 May 2013 / Published online: 21 May 2013

Abstract Present work reports the structural, optical and ferroelectric properties of vanadium doped ZnO samples synthesized via solid state reaction method. X-ray diffraction (XRD) study confirms the presence of hexagonal wurtzite phase and the slight changes in lattice parameters is observed after V doping in host ZnO and impurity oxide of ZnV_2O_6. Presence of E_1 and E_2 modes in Raman spectroscopy of V doped ZnO indicates the stability of the wurtzite structure of ZnO, which is consistent with the XRD results. UV–Vis spectroscopy results show decrease in band gap of ZnO from 3.35 to 3.24 eV for 1 % V doped sample, whereas it increases with the V doping and increase in the impurity of ZnV_2O_6. Furthermore, it is observed that the ferroelectric polarisation of ZnO improves by V doping. Above results show that one need to consider the presence of ZnO in composite form of oxides of Zn and V and not as a pure V doped ZnO system.

Keywords Zinc oxide · Raman spectroscopy · Ferroelectricity and hysteresis curve

R. Joshi · A. Gaur
Department of Physics, National Institute of Technology, Kurukshetra 136 119, India

P. Kumar
Department of Physics, Indian Institute of Technology Delhi, New Delhi 110 016, India

K. Asokan (✉)
Material Science Division, Inter University Accelerator Centre, New Delhi 110 067, India
e-mail: asokan@iuac.res.in

Introduction

Doping results in dramatic changes in the structural, optical, electrical and magnetic properties of wide band gap semiconductors. ZnO and oxides of vanadium exhibit multifunctional properties that make them interesting materials for technological applications. Zinc oxide has wide band gap (3.3 eV) and large exciton binding energy (60 meV) which makes it suitable for short wavelength optoelectronic devices (Wang 2004; Kumar et al. 2012). Doping these metal oxides enhances the magnetic, optical and semiconducting properties (Karamat et al. 2010). Vanadium doped ZnO attracted researchers because of improved electric and magnetic properties (Schlenker et al. 2007; Naydenova et al. 2010). Single phase ZnO–V_2O_5 system has been considered as a diluted magnetic semiconductor (DMS) material. The existence of ferromagnetism in V doped ZnO was theoretically predicted by Sato and Yoshida (2002). For electrical properties, V ions replace the Zn^{2+} site in ZnO lattice to compensate the electric charge and results in the enhancement in electron concentration of the system. The increased electron concentration gives rise to an increase in the electrical conductivity (Jin et al. 2000). Apart from the improved ferromagnetic and electrical properties, V doped ZnO exhibits good ferroelectric nature at and above room temperature, which adds an additional dimension to its applications (Schlenker et al. 2007; Naydenova et al. 2010). Till date, the ferroelectric materials used for ferroelectric memory devices are mainly based on perovskite ferroelectrics that are structurally complicated and relatively difficult to synthesize. Furthermore, some ZnO-based ferroelectric materials have also been reported. However, the problem in ZnO-based ferroelectrics (Li, Mg and Cr-doped ZnO) is their low remnant polarization and high coercive

field (Onodera et al. 1996; Kumar et al. 2013; Dhananjay et al. 2006; Yang et al. 2008). The persistence of ferroelectric behaviour, at and above room temperature in V doped ZnO opens up new possibilities for high temperature nanopiezotronics applications and ferroelectric memory devices.

In view of the above, present study focuses the physical properties of V doped ZnO. We have synthesized pure ZnO, 1, 5 and 9 % V doped ZnO samples by solid state reaction method and studied their structural, morphological, optical and ferroelectric properties by characterising them through X-ray diffraction, Raman, UV–Vis spectroscopy and ferroelectric loop tracer.

Experimental

ZnO and 1, 5, and 9 % V doped ZnO samples were prepared by solid state reaction using V_2O_5 and ZnO as initial precursors. Appropriate amount of precursors, ZnO and V_2O_5 powders were mixed together and ground for 2 h for the proper mixing of powder. The ground powder was then calcined at 700 °C for 8 h, again ground and pelletized. These pellets were again sintered at 800 °C for 14 h to remove the lattice defects. The synthesized samples were characterized by various techniques for their structural, optical and ferroelectric properties. Bruker D8 X-ray Diffractometer was used for structural investigations and surface morphology was investigated using scanning electron microscope (SEM), MIRA II LMH, TESCAN. Raman spectroscopy was performed with InVia Raman microscope (Renishaw) with Ar^+ ion laser beam having wavelength of 514 nm and 50 mW power. Ferroelectric hysteresis loops were measured using ferroelectric loop tracer.

Results and discussion

X-ray diffraction (XRD)

XRD patterns of V doped ZnO samples are shown in Fig.1. All the diffraction peaks in the pattern can be indexed using pure wurtzite phase of ZnO with hexagonal structure (JCPDS database of card number 36-1451). It is clear from the figure that all the samples doped with different amounts of V have similar crystal structures. An impure phase corresponding to ZnV_2O_6 was also found which is marked as * in the XRD patterns for V doped ZnO samples. As evident from Fig. 1, as the concentration increases, the intensity of these peaks assigned to impurity phases also increases. The same phases are also found at all higher doping levels of V. There is a slight variation in the lattice parameter '*a*' whereas significant increase in the lattice parameter '*c*' with increasing the doping concentration (Table 1). This change in lattice parameter values is attributed to larger ionic radii of V^{2+} (0.93 Å) ions compared to that of the Zn^{2+} (0.60 Å) ions. Doping V causes distortion in the ZnO crystal structure. Factors like non-uniform distribution of dopants, deviation of V from divalent state may also cause decrease in value of lattice parameter. Similar kinds of behaviour, i.e. decrease in lattice parameter after a particular doping concentration is also reported by other authors (Karamat et al. 2010; Yang et al. 2008).

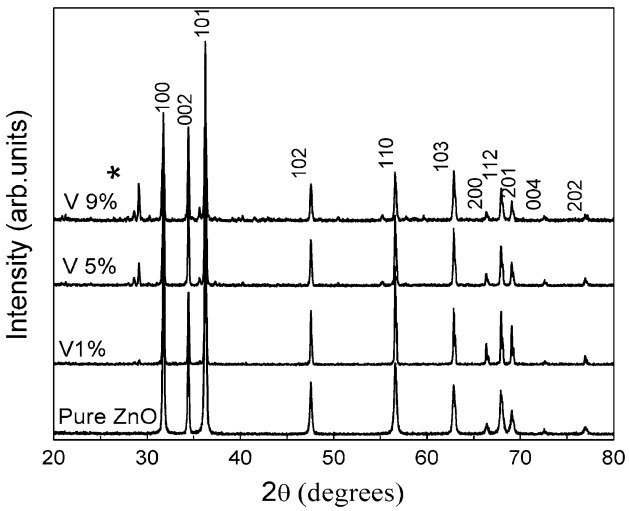

Fig. 1 XRD pattern of V doped ZnO samples, where * represents the impure phase corresponding to ZnV_2O_6

The average crystallite size for all the samples was determined from the broadening of XRD peaks using the Scherer's formula ($D = 0.89\lambda/\beta \cos\theta$). Where D is crystallite size, β is FWHM and λ is the wavelength of X-rays used. The crystallite size for pure ZnO is estimated to be ~45 nm, which found to be varying from 50 to 60 nm by increasing the V content.

Scanning electron microscopy SEM

The surface morphology of V doped ZnO with various concentrations examined by SEM are shown in Fig. 2a–d. The average particle size increases with the increase in concentration of V ions. The average particle size for pure ZnO is 0.48 μm and it increase with the increase in V content (~1.3, ~1.9 and ~1.8 μm corresponding to 1, 5 and 9 % V content). For lower concentration (1–5 %), the homogeneity can be seen but for higher concentration inhomogeneous distribution is evident. As doping concentration is large, it causes inhomogeneity and destroys the crystal structure (Wang et al. 2009) as can be observed for 9 % doped sample. There is a large difference in particle size of pure and the 1 % V doped sample which

Table 1 Parameters for vanadium doped ZnO samples

Composition	*a* (Å)	*c* (Å)	*c*/*a* ratio	Cell volume (Å^3)	Band gap (eV)
Pure ZnO	3.2499	5.2038	1.6012	47.59	3.35
1 % V doped ZnO	3.2500	5.2055	1.6016	47.61	3.24
5 % V doped ZnO	3.2512	5.2063	1.6013	47.66	3.25
9 % V doped ZnO	3.2505	5.2059	1.6015	47.63	3.30

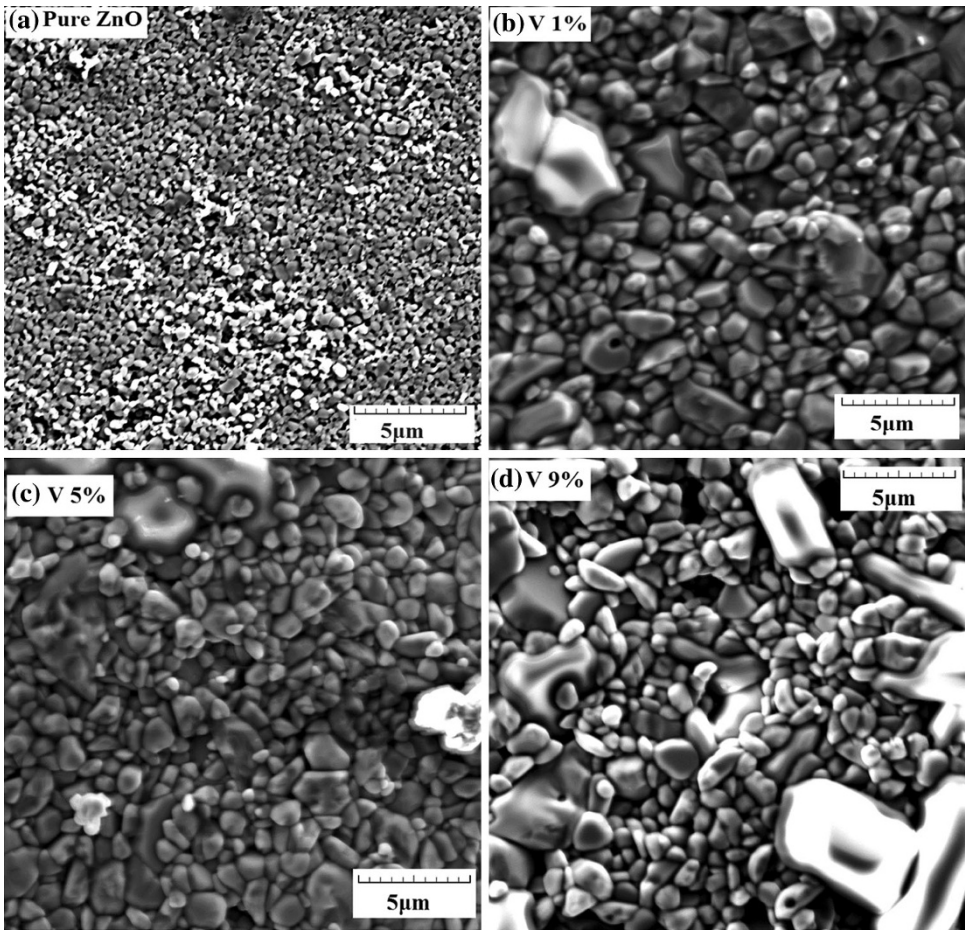

Fig. 2 Scanning Electron Micrographs (SEM) of V doped ZnO samples

indicates that even a small amount of V doping causes a significant change in the morphology. This may be due to the substitution of Zn^{2+} by V ion, which causes distortion in system and increases the activity of ZnO. This increased activity helps in grain growth and formation of bigger particles in V doped ZnO samples (Colak and Turkoglu 2012). Since the ionic radii mismatch is quite higher in this case, it causes significant increase in the particle size even at very small doping concentration.

Raman spectroscopy

To obtain detailed information about the structural composition of doped samples, Raman spectroscopy measurements were performed. The hexagonal wurtzite ZnO structure belongs to the space group P_63mc. The optical phonon mode for ZnO according to the group theory can be expressed as:

$$\Gamma_{\text{Optic}} = A_1 + 2B_1 + E_1 + 2E_2.$$

The modes corresponding to A_1 and E_1 symmetry are polar phonons and are infrared active whereas the E_2 modes are non-polar and Raman active. The B_1 modes are known as the silent modes as these are infrared and Raman inactive. The polar modes exhibit different wave numbers for the transverse optical (TO) and longitudinal optical (LO) phonons. The non-polar phonon modes E_2 split as E_2 (high), associated with oxygen atoms and E_2 (low), associated with Zn sub lattice (Ashkenov et al. 2003; Damen et al. 1966).

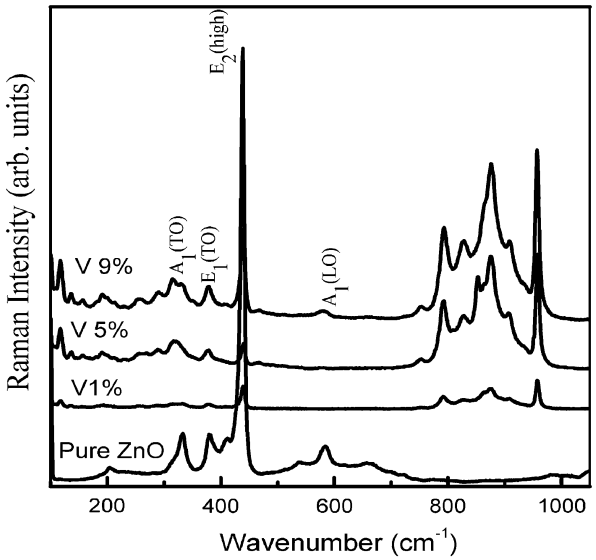

Fig. 3 Raman spectra of V doped ZnO samples

Figure 3 shows the Raman spectra for all the samples in the range of 100–1,000 cm^{-1}. Several peaks were observed in doped samples at 117, 193, 330, 379, 438, 793, 831, 874, 903, and 957 cm^{-1}. The peak at 438 cm^{-1} is the characteristic peak of ZnO which corresponds to the E_2 (high) vibrational mode and band characteristic of wurtzite crystal structure (Youn et al. 2004). It is evident that there are several peaks in addition to the pure ZnO modes. The peaks in the range of 100–330 cm^{-1} are related to the oxides of V modes and are mostly from the lattice and bending modes of V–O. The peaks in the range of 780–1,000 cm^{-1} are mainly due to the ZnO and impurity phases of V doping. In lower wave number region, the peak at 330 cm^{-1} corresponds to transverse optical (TO) phonons of A_1 mode which is second order Raman mode (Samanta et al. 2006). Some defects like oxygen vacancies, Zn interstitials give rise to A_1 mode. On the other hand, the phonons corresponding to the E_1 mode were also observed, the peak at 379 cm^{-1} corresponds to E_1 (TO) mode. A_1 or E_1 modes in Raman spectra indicate that the lattice vibrations in crystal lattice or in sample are parallel or perpendicular to the c-axis, respectively. It is also supported by the longitudinal and transverse optical emission of phonons (Youn et al. 2004).

There is a significant shift in peak position at 379 and 439 cm^{-1} towards lower wave numbers corresponding to E_1 (TO) and E_2 (high) modes, respectively. These modes are characteristic of ZnO and these are also present in V doped ZnO. Some Raman peaks are also observed towards lower frequencies at 136 and 190 cm^{-1} especially for higher concentration, appear due to the stretching mode of $(V_2O_2)_n$ which correspond to the chain translation (Juloen et al. 1997). The peak at 255 cm^{-1} is broad in nature and may be due to V–O–V bending mode (Wang et al. 2001). Actually this peak consists of more than one peak. The peak at 315 cm^{-1} assigned to triply coordinated oxygen (V_3–O) bond and stretching band (Chen et al. 2004). There are many modes in the wave number range of 750–1,000 cm^{-1} arise due to V doping in ZnO. The absence of these modes in pure ZnO spectra shows that these modes are associated with the vanadium.

UV–Visible spectroscopy

The optical band gap was calculated by extrapolation of linear portion of α^2 versus $h\nu$ by using the Tauc's relation (Tauc 1971), given by $(\alpha h\nu) = (h\nu - E_g)^{1/2}$. Here, α is the absorption coefficient, $h\nu$ is the energy of the radiation (photon energy), E_g is the optical band-gap of the materials. Therefore, the absorption coefficient (α) is given by

$$\alpha = 2.303 \log_{10}(A)/t$$

where A is the absorbance and t is the thickness of pellets. Figure 4 explains the variation of $(\alpha h\nu)^2$ versus photon energy ($h\nu$) for all the samples. The band gap for pure ZnO is found to be $E_g \approx 3.35$ and for V doped ZnO samples of 1, 5 and 9 % V, it is 3.24, 3.25 and 3.30 eV, respectively. It can be seen (Table 1) that the band gap of all the V doped samples is lower than the pure ZnO sample. The reason for this decrease in band gap may be explained on the basis of alloying effect between ZnO and V_2O_5. The band gap of V_2O_5 is 2.3 eV and ZnO is 3.37 eV. When V_2O_5 is doped in ZnO, mixed oxide of ZnV_2O_6 is formed and causes the decrease in the band gap. However, increase in doping concentration led to increase in band gap value which indicates that the Burstein–Moss effect is dominating for higher concentrations.

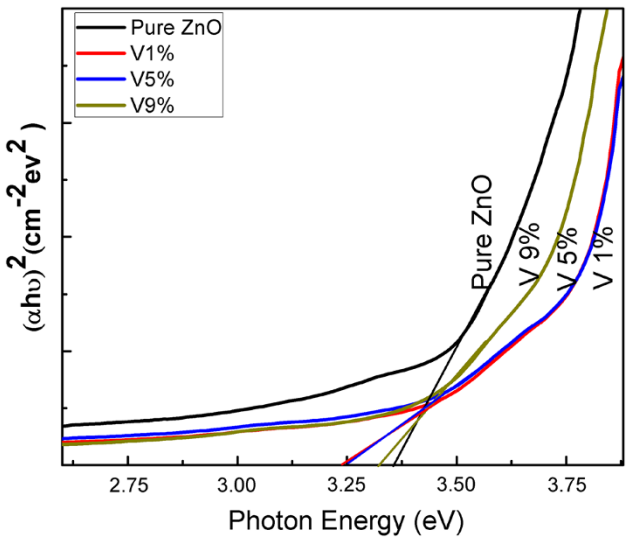

Fig. 4 Tauc's plot for V doped ZnO samples

It is observed that the band gap of these samples increases with the doping concentration. This might be due to the influence of many factors such as structural parameters, carrier concentrations and presence of defects such as oxygen vacancies which may lead to the Burstein–Moss shift (Yang et al. 2008; Tahir et al. 2009). The Burstein–Moss effect is the process by which the apparent band gap of a semiconductor is increased as the absorption edge is pushed to higher energies as a result of all states close to the conduction band being populated. In Burstein–Moss effect, the Fermi level merges into the conduction band because the addition of V in ZnO contributes electrons to the conduction band. The band gap of pure ZnO is $E_g \approx 3.35$ and the band gap of V doped ZnO samples is smaller than this and is found to be 3.24, 3.25 and 3.30 eV corresponding to 1, 5 and 9 % V content. The reason for this decrease in band gap may be explained by the alloying effect between V_2O_5 and ZnO. As the band gap of V_2O_5 is 2.3 eV and ZnO is 3.37 eV, when V_2O_5 is doped in ZnO, alloy is formed and causes decrease in band gap. It is clear from Table 1 that for 1 % doping the band gap is lowest, but as the doping concentration increases, the band gap increases instead of decreasing which indicates that the Burstein–Moss effect is dominating for higher concentrations.

Ferroelectric hysteresis (P–E loop)

Room temperature ferroelectric hysteresis curves at an applied external field of 5 kV/cm for V doped ZnO are shown in Fig. 5. The hysteresis curves of all samples show loose unsaturated ferroelectric behaviour, however the value of maximum polarization (P_{max}) increases with the doping of V in host ZnO from 1.68 to 3.73 μC/cm^2. The ferroelectric behaviour originates from the dipole orientation. When there is no field applied, the dipoles will have random orientation and as a result there will be no ferroelectric behaviour. On the other hand with the application of electric field, dipoles align themselves along the field direction resulting in polarization.

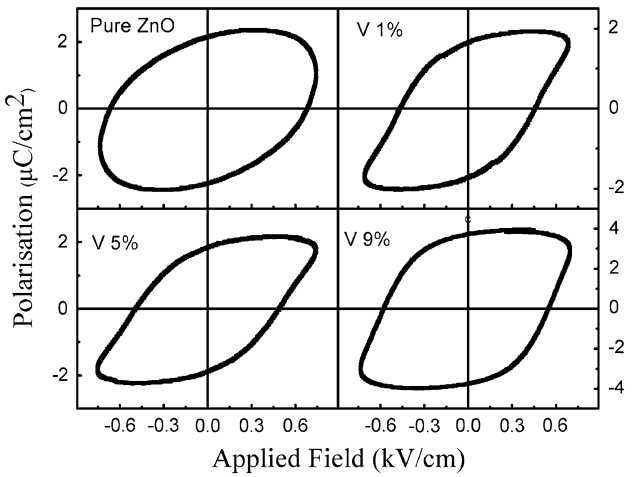

Fig. 5 Hysteresis curves of V doped ZnO samples

In the case of II–VI semiconductors, the ferroelectricity is believed to be originating from the off-centred position of cations. The ionic radii of Zn^{2+} (0.74 Å) and the dopant ion V^{2+} (0.93 Å) ions are different. Therefore V^{2+} ion occupies the off-centred positions and gives rise to permanent local electric dipoles (ferroelectric behaviour) on the application of electric field (Onodera et al. 1996). Apart from off-centred distortion, V substitution on Zn site breaks some Zn–O bonds and formation of new V–O bond takes place. These V–O bonds are non collinear and can rotate easily with the application of external field (Gupta and Kumar 2011). Apart from this, the V–O bond has stronger polar nature than Zn–O (Yang et al. 2007). Therefore the off-centred distortion and the formation of additional V–O bonds will result in the improvement in ferroelectric nature after V incorporation.

Conclusions

In summary, we have synthesized the V doped ZnO samples by solid state reaction method and investigated their structural, optical and ferroelectric properties. It has been found that the lattice parameter slightly increases after V doping, indicating partial substitution in host matrix. The shifting in Raman modes of pure ZnO after V incorporation also indicates the presence of V ions in the host matrix. UV–Vis study shows that the band gap of ZnO decreases from 3.35 to 3.24 eV for the 1 % V doped sample. Moreover, P–E loop study reveals that pure ZnO sample exhibit weak ferroelectricity which is slightly improved by V doping.

Acknowledgments Authors (R.J. and P.K.) would like to acknowledge Inter University Accelerator Centre (IUAC), New Delhi for providing experimental facility and also acknowledge the experimental support of Dr. Gagan Dixit and Dr. Yogesh Kumar during this project and fruitful discussion.

References

Ashkenov N, Mbenkum BN, Bundesmann C, Riede V, Lorenz M, Spemann D, Kaidashev EM, Kasic A, Schubert M, Grundmann M (2003) Infrared dielectric functions and phonon modes of high-quality ZnO films. J Appl Phys 93:126

Chen W, Mai L, Peng J, Xu Q, Zhu Q (2004) Raman spectroscopy study of vanadium oxide nanotubes. J Solid State Chem 177:377–379

Colak H, Turkoglu O (2012) Synthesis, crystal structural and electrical conductivity properties of Fe-doped zinc oxide powders at high temperatures. J Mater Sci: Mater Electron 28(3):268–274

Damen TC, Porto SPS, Tell B (1966) Raman Effect in Zinc Oxide. Phys Rev 142:570–574

Dhananjay, Krupanidhi SB (2006) Dielectric properties of c-axis oriented $Zn_{1-x}Mg_xO$ thin films grown by multimagnetron sputtering. Appl Phys Lett 89:082905(1–3)

Gupta MK, Kumar B (2011) High T_c ferroelectricity in V-doped ZnO nanorods. J Mater Chem 21:14559–14562

Jin Z, Murakami M, Fukumura T, Matsumoto Y, Ohtomo A, Kawasaki M, Koinuma H (2000) Combinatorial laser MBE synthesis of 3d ion doped epitaxial ZnO thin films. J Cryst Growth 55:214–215

Juloen C, Nazri GA, Bergstrom O (1997) Raman Scattering Studies of Microcrystalline V_6O_{13}. Phys Stat Solidi B 201:319–326

Karamat S, Rawat RS, Lee P, Tan TL, Ramanujan RV, Zhou W (2010) Structural, compositional and magnetic characterization of bulk V_2O_5 doped ZnO system. Appl Surf Sci 256:2309–2314

Kumar P, Singh JP, Kumar Y, Gaur A, Malik HK, Asokan K (2012) Investigation of phase segregation in $Zn_{1-x}Mg_xO$ systems. Curr Appl Phys 12:1166–1172

Kumar P, Kumar Y, Malik HK, Annapoorni S, Gautam S, Chae KH, Asokan K (2013) Possibility of room temperature multiferroism in Mg Doped ZnO. Appl Phys A. doi:10.1007/s00339-013-7664-9

Naydenova T, Atanasov P, Koleva M, Nedialkov N, Perriere J, Defourneau D, Fukuoka H, Obara M, Baumgart C, Zhou S, Schmidt H (2010) Influence of vanadium concentration on the microstructure and magnetic properties of V-doped ZnO thins films. Thin Solid Films 518:5505–5508

Onodera A, Tamaki N, Kawamura Y, Sawada T, Yamashita H (1996) Dielectric activity and ferroelectricity in piezoelectric semiconductor Li-doped ZnO. Jpn J Appl Phys 35:5160–5162

Samanta K, Bhattacharya P, Katiyar RS (2006) Raman scattering studies in dilute magnetic semiconductor $Zn_{1-x}Co_xO$. Phys Rev B 73(245213):1–5

Sato K, Karayama-Yoshida H (2002) First principles materials design for semiconductor spintronics. Semicond Sci Technol 17:367–376

Schlenker E, Bakin A, Postels B, Mofor AC, Kreye M, Ronning C, Sievers S, Albrecht M, Siegner U, Kling R, Waag A (2007) Magnetic characterization of ZnO doped with vanadium. Superlattices Microst 42:236–241

Tahir N, Hussain ST, Usman M, Hasanain SK, Mumtaz A (2009) Effect of vanadium doping on structural, magnetic and optical properties of ZnO nanoparticles. Appl Surf Sci 255:8506–8510

Tauc J (1971) Amorphous and liquid semiconductors. Plenum Press, London

Wang ZL (2004) Zinc oxide nanostructures: growth, properties and applications. J Phys: Condens Matter 16:R829–R858

Wang XJ, Li HD, Fei YJ, Weng X, Xiong YY, Nie YX, Feng KA (2001) XRD and Raman study of vanadium oxide thin films deposited on fused silica substrates by RF magnetron sputtering. Appl Surf Sci 177:8–14

Wang L, Meng L, Teixeira V, Song S, Xu Z, Xu X (2009) Structure and optical properties of ZnO:V thin films with different doping concentrations. Thin Solid Films 517:3721–3725

Yang YC, Song C, Zeng F, Pan F, Xie YN, Liu T (2007) Giant piezoelectric d33 coefficient in ferroelectric vanadium doped ZnO films. Appl Phys Lett 90(42903):1–3

Yang YC, Song C, Wang XH, Zeng F, Pan F (2008) Cr-substitution-induced ferroelectric and improved piezoelectric properties of $Zn_{1-x}Cr_xO$ films. J Appl Phys 103:074107 (1–6)

Youn CJ, Jeong TS, Han MS, Kim JH (2004) Optical properties of Zn-terminated ZnO bulk. J Cryst Growth 261:526–532